

REDUCTION OF CORRUGATION BY SEMI-ACTIVE TRACK

O.Vaculín¹, M. Valášek², and A. Preumont³

¹ Deutsches Zentrum für Luft- und Raumfahrt e.V. (DLR)
Institute of Robotics and Mechatronics
Vehicle System Dynamics
PO Box 1116, D-82230 Wessling, Germany
e-mail: Ondrej.Vaculin@DLR.de, web page: <http://www.ae.op.dlr.de>

² Czech Technical University in Prague (CTU)
Faculty of Mechanical Engineering
Department of Mechanics
Karlovo nám. 13, 121 35 Praha 2, Czech Republic
e-mail: valasek@fsik.cvut.cz, web page: <http://www.mechatronics.cz>

³ Free University of Brussels, (ULB)
Active Structures Laboratory
C.P. 165/42
AV. F.D. Roosevelt 50, B-1050 Bruxelles, Belgium
e-mail: Andre.Pneumont@ulb.ac.be, web page: <http://www.ulb.ac.be/scmero>

Keywords: rail corrugation, semi-active rail pads, control, optimization, simulation.

Abstract. *This article discusses possibilities for application of semi-active actuators to reduce rail and wheel wear. A simple model of a vehicle/track interaction is presented. The model is extended with a model of semi-active actuators. The feedback control law is proposed and optimised and the simulations are compared to the passive model.*

1 INTRODUCTION

The wear is of major concern for almost every railway and vehicle maintenance authority, since re-profiling and replacing worn wheels and rails absorbs a significant part of the maintenance budget. The financial impact due to wear of the rails in the European Community is estimated at 300 million Euro per year. Furthermore, the worn rails cause additional deterioration of the rail vehicles and vice versa. Some increase of traction energy consumption with regard to the wear is also reported and last but not least the increase of noise and vibration level is observed. The wear can be divided into several

categories based on the result of the wear, such as homogenous wear, wavelike wear, flats, fatigue, etc.

Periodical wavelike deformations occur frequently on the rail surface due to high contact vibration with slips. This phenomenon is called corrugation. It causes serious noise and vibration and significant problems in railway vehicle operation.

Some hypotheses on the corrugation formation are presented in literature [1, 2, 3]. The corrugation could occur as a result of longitudinal slip between wheel and rail and is supported by the variation of track impedance (stiffness and damping of the track). Some eigenmodes of the vehicle-track system are excited resulting in corrugation wear.

In order to reduce the corrugation, one should focus on the trackside or on the wheelset/primary suspension side. An application of semi-active damping of track is proposed. The simulation results described in [4] indicate an influence of passive track parameters to the corrugation. Further improvement can be achieved by application of control devices. No need for high-power supply and relative simplicity of installation encourage the semi-active systems.

The dynamic of semi-active actuators play a critical role, since the frequencies to be damped are rather high. The time constants are required to be in the range of milliseconds.

2 CORRUGATION MODEL

According to Diana et al., [1], the variation of track impedance (stiffness and damping) plays an important role in the corrugation formation. The model presented in this paper verifies this hypothesis is based on model from [1]. The model is rather simplified; it includes only the essential features of the corrugation formation: torsional and bending modes of the wheelset and variation of the track stiffness. It consists of a dynamic model of the vehicle and the track, a model of the rail irregularities, and a simple evaluation of the wear rate.

2.1 Dynamic Model of Vehicle and Track

2.1.1 Structure

The model has 3 degrees of freedom. It takes into account a single bending mode z_w , a torsional degree of freedom of the wheelset producing creepage φ , and a degree of freedom representing the vertical motion of the track z_t . A draft of the model is presented in Figure 1. The parameters m_w , b_s and k_s represent the modal parameters of the bending mode of the wheelset, J_w , b_φ and k_φ are the modal parameters of the torsional degree of freedom and m_t , b_t and $k_t(\xi)$ represent the track parameters. The track impedance variation is represented by the track stiffness variation:

$$k_t(\xi) = k_{t0} + \Delta k_t(\xi), \quad (1)$$

where k_{t0} is the mean value and $\Delta k_t(\xi)$ is a periodic function of the wheelset position ξ . The wheel/rail contact is represented by the stiffness k_c and damping b_c . The track vertical irregularity is denoted by $h(\xi)$.

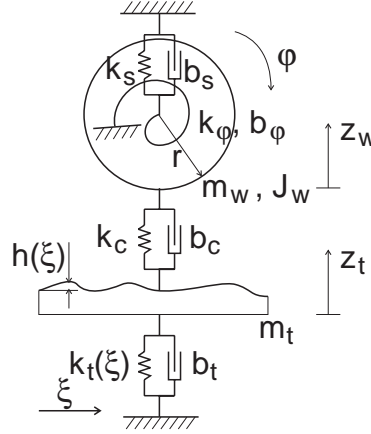


Figure 1: Schematic draft of model according to [1]

A pre-load is set to the torsional degree of freedom in order to reproduce the saturation regime of contact forces, which is believed to be a cause of the corrugation. It could represent a driving moment from e.g. a drive motor during acceleration. Lateral degree of freedom is not included in order to keep the model simple.

2.1.2 Equations of Motion

The equations of motion based on the Newton-Euler approach, [5], for the model form Figure 1 are:

$$\begin{aligned}
m_w \ddot{z}_w &= -(b_s + b_c) \dot{z}_w + b_c \dot{z}_t - (k_s + k_c) z_w + k_c z_t + b_c \dot{h}(\xi) + k_c h(\xi), \\
m_t \ddot{z}_t &= b_c \dot{z}_w - (b_c + b_t) \dot{z}_t + k_c z_w - (k_c + k_{t0}) z_t - b_c \dot{h}(\xi) \\
&\quad - k_c h(\xi) - \Delta k_t(\xi) z_t - \Delta k_t(\xi) z_{t0}, \\
J_w \ddot{\phi} &= -b_\phi \dot{\phi} - k_\phi \phi - (T_c - T_{c0}) r,
\end{aligned} \tag{2}$$

where

z_0 is the average static deflection of the track under wheel load P ,

T_{c0} is the longitudinal contact force corresponding to the torsional pre-load,

T_c is the dynamic longitudinal force and

r is the wheel radius.

The dynamic longitudinal force is:

$$T_c = -\mu N, \tag{3}$$

where μ is the creep coefficient and N is the normal force.

The creep coefficient is expressed as follows:

$$\mu = \frac{f_{11}\varepsilon}{\sqrt{1 + \left(\frac{f_{11}\varepsilon}{\mu_{\max}}\right)^2}}, \quad (4)$$

where ε is the dynamic component of creepage and f_{11} is the linear creep coefficient.

The normal force N is:

$$N = P - b_c \dot{z}_w + b_c \dot{z}_t + b_c \dot{h}(\xi) - k_c z_w + k_c z_t + k_c h(\xi), \quad (5)$$

where P denotes the static wheel load.

The dynamic component of creepage is:

$$\varepsilon = -\frac{r\dot{\varphi}}{v}, \quad (6)$$

where v represents the vehicle velocity.

2.1.3 Model States, Inputs and Outputs

The ordinary differential equations (ODEs) of the first order are necessary for the model implementation to MATLAB/Simulink. The states chosen for the set of the first order ODEs are presented in Table 1.

$x(1)$	z_w	wheel bending position
$x(2)$	\dot{z}_w	wheel bending velocity
$x(3)$	z_t	track vertical position
$x(4)$	\dot{z}_t	track vertical velocity
$x(5)$	φ	wheel torsional angle
$x(6)$	$\dot{\varphi}$	wheel torsional velocity

Table 1: Model states

The model has 3 inputs: (i) height of the rail irregularity, (ii) its first derivative, and (iii) variation of the track stiffness, see Table 2, and eight outputs: all six states (Table 1), the longitudinal force $T_c - T_{c0}$ and the creepage ε .

$u(1)$	$h(\xi)$	rail irregularity
$u(2)$	$\dot{h}(\xi)$	velocity of rail irregularity
$u(3)$	$\Delta k_t(\xi)$	variation of track stiffness

Table 2: Model inputs

2.2 Model of Rail Irregularities and Track Impedance Variation

2.2.1 Rail Irregularities

In order to excite the vehicle model, stochastic rail irregularities are chosen. The rail irregularities generation is similar to previous projects, [6]. The stochastic rail excitation is realised as a sum of 255 harmonic functions. The amplitudes and phases are dependent on the length frequency in $[1/m]$. This type of generation of quasi-stochastic track profiles is more suitable for nonlinear simulations than direct filtering of white noise. The transfer function of the filter is defined as follows:

$$F(j\Omega) = \frac{b_0 + b_1 j\Omega}{a_0 + a_1 j\Omega + (j\Omega)^2}, \quad (7)$$

where

b_i are the coefficients of the numerator,

a_i are the coefficients of the denominator,

j is the imaginary unit,

Ω is the frequency $[rad/m]$ given in the distance domain.

The transfer function parameters are taken from the SIMPACK documentation, [7], for “DB - vertical - high level type” of the excitation. Since the numerical integration is performed in the time domain, the filter parameters are re-calculated from the distance domain to the time domain.

2.2.2 Track Stiffness Variation

The track impedance variation is modelled as harmonic variation of the track stiffness Δk_t , which has the amplitude of 30 % of the static stiffness k_t :

$$\Delta k_t = 0.3k_t \sin(\omega_{\Delta k} t). \quad (8)$$

The angular frequency of the impedance variation $\omega_{\Delta k}$ is defined in the time domain as follows:

$$\omega_{\Delta k} = 2\pi \frac{v}{d}, \quad (9)$$

where v is the vehicle velocity, and d is the distance of the sleepers.

2.3 Abrasion

In order to evaluate the rail wear, a measure proportional to the abrasion rate is introduced. According to [8] the rate of abrasion w is assumed to be proportional to:

$$w = T \cdot \varepsilon, \quad (10)$$

where ε is the creepage from (6), and T is the tangential (longitudinal) force:

$$T = T_c - T_{c0}, \quad (11)$$

where T_c is the dynamic longitudinal force from (3), and T_{c0} is the longitudinal contact force corresponding to the torsional pre-load.

2.4 Parameters

The model should represent an vehicle of Brussels public transport company STIB/MIVB¹. The parameters available from STIB/MIVB (e.g. wheel radius, wheelset mass, static load) are used in the model. Further parameters are estimated based on parameters of similar vehicles published in literature, [1, 9, 10] (e.g. wheelset eigenfrequencies, moment of inertia, track mass, stiffness and damping, wheel/rail contact model coefficients, etc.).

2.5 Implementation

The model is implemented in MATLAB/Simulink environment. The Simulink block diagram of the model is presented in Figure 2.

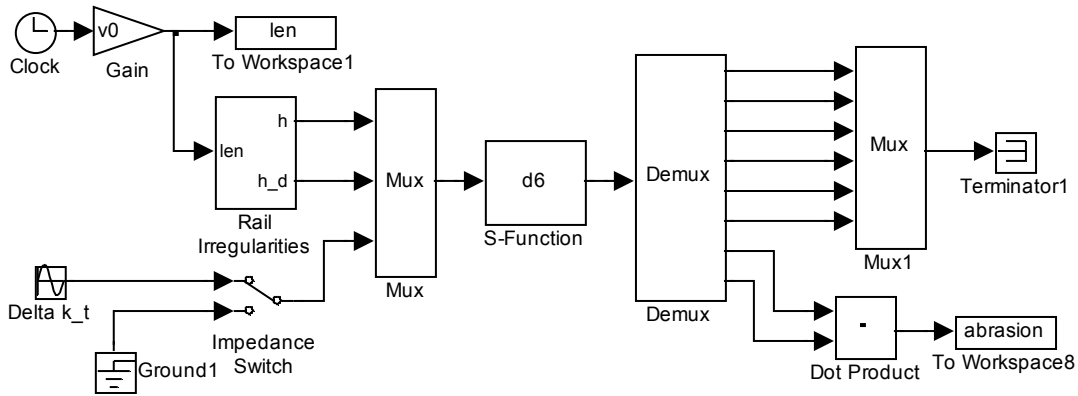


Figure 2: Simulink block diagram of model

The set of the nonlinear differential equations (2) describing the vehicle is implemented in the block `d6` as a Simulink S-function in MATLAB language. The stochastic rail irregularity generator implemented in the block `Rail Irregularities` is a Simulink S-function as well. The realisation of the stochastic rail irregularities $h(\xi)$ is presented in Figure 3. The harmonic track stiffness variation $\Delta k_t(\xi)$ generated by the block `Delta_k_t` is shown in Figure 4.

¹ Société des Transports Intercommunaux de Bruxelles/Maatschappij voor Intercommunaal Vervoer van Brussel

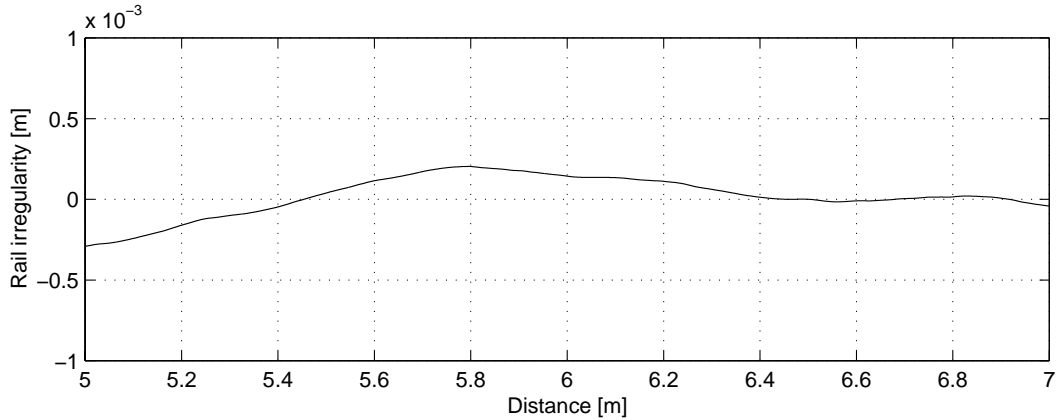
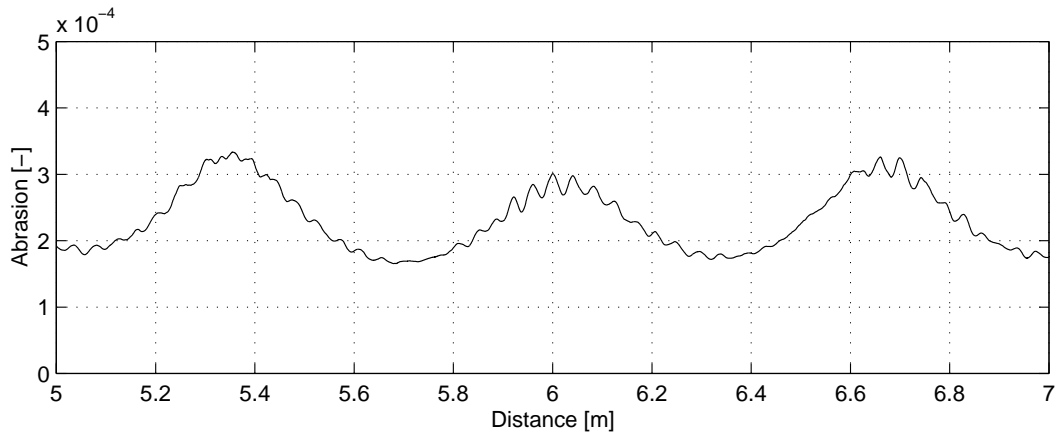


Figure 3: Realisation of stochastic rail irregularities

Figure 4: Track stiffness variation $\Delta k_t(\xi)$

Selected outputs are saved to the MATLAB workspace for further post-processing. Since the simulation is performed in the time domain, the distance is calculated and stored to the workspace, too.

3 SIMULATION RESULTS

The simulations have been performed at a velocity of 15 m/s (54 km/h) for simulation time 0.5 s (7.5 m). Two basic simulation experiments have been performed: without and with the stiffness variation. The results are presented in Figures 5 and 6. Because of transient effects at the beginning, the responses are evaluated for the track between the 5th and 7th meter. Figure 5 shows the abrasion rate in the case with constant track stiffness, the model is excited only by rail irregularities.

The abrasion rate with track stiffness harmonic variation is depicted in Figure 6. The influence of the stiffness variation on the abrasion rate is evident. The mean value is more

than twice as high. Moreover, the abrasion rate is significantly modulated by the variation of the track stiffness, and even high frequency components are more excited than in the case of constant track impedance. These high frequency oscillations form the corrugation of the wavelength about 5 cm. The wavelength corresponds to the frequency of the torsional eigenmode of the wheelset (about 300 Hz) for the given velocity.

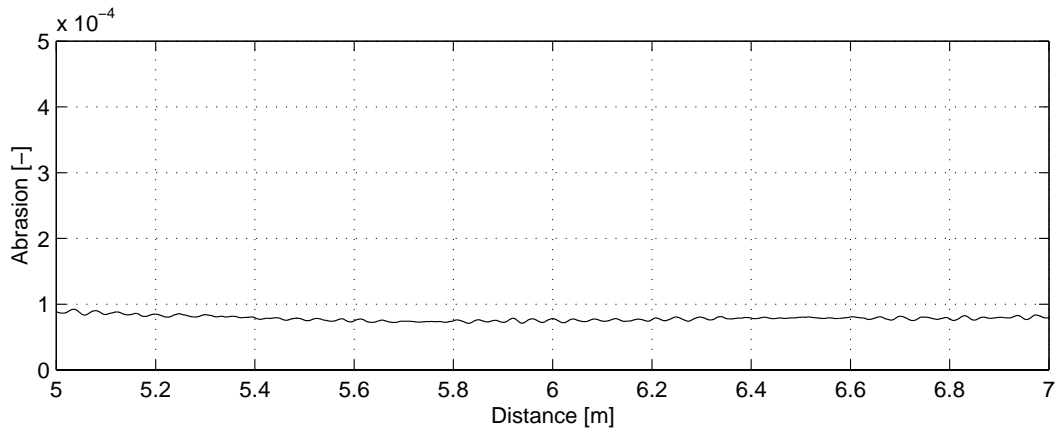


Figure 5: Abrasion rate, constant track stiffness, stochastic rail excitation

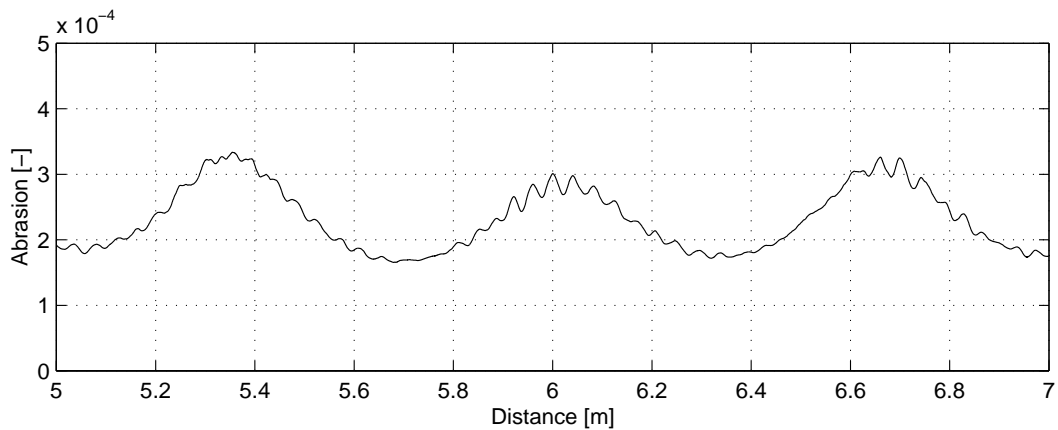


Figure 6: Abrasion rate, variable track stiffness, stochastic rail excitation

In order to identify the influence of the stochastic rail excitation, the simulation experiment with rail irregularities reduced to 1/10 has been performed (e.g. rail after grinding). The abrasion rates are available in Figures 7 and 8. The ratio between the track with and without the impedance variation is not as dramatic as in the previous case.

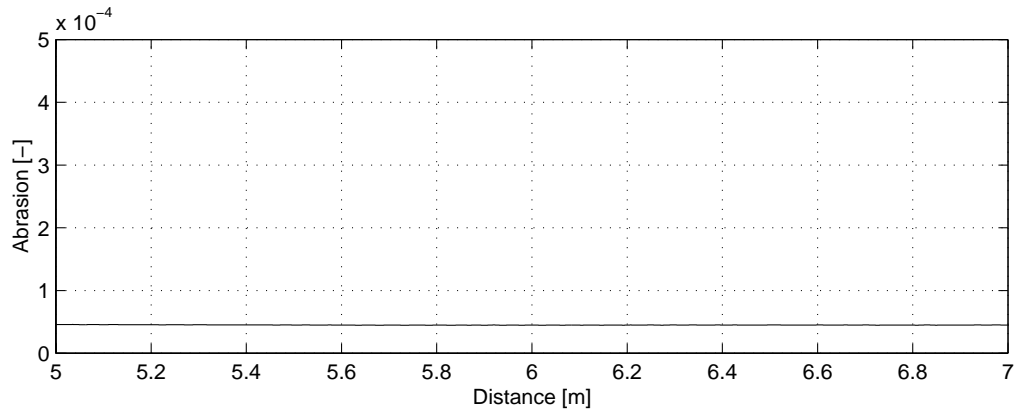


Figure 7: Abrasion rate, constant track stiffness, no rail irregularities

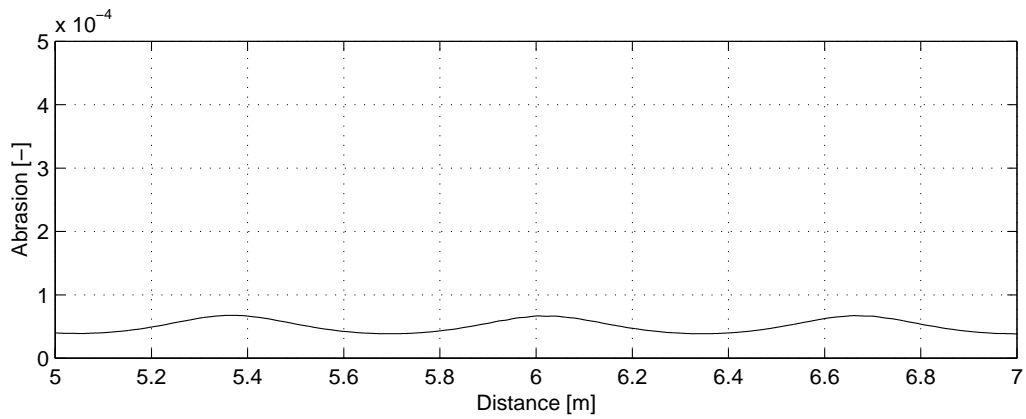


Figure 8: Abrasion rate, variable track stiffness, no rail irregularities

4 SEMI-ACTIVE TRACK

The approach based on controllable track parameters cannot be applied throughout the whole track, but only at the most critical areas, such as acceleration and braking areas or low radius curves, particularly those in which the vibrations are transmitted through the soil to the buildings.

4.1 Model Modifications

In order to simulate the influence of semi-active sleepers on the rail wear, the model presented in previous sections is modified and extended with a model of a semi-active damping device in the track part. The Simulink block diagram of the modified model is presented in Figure 9.

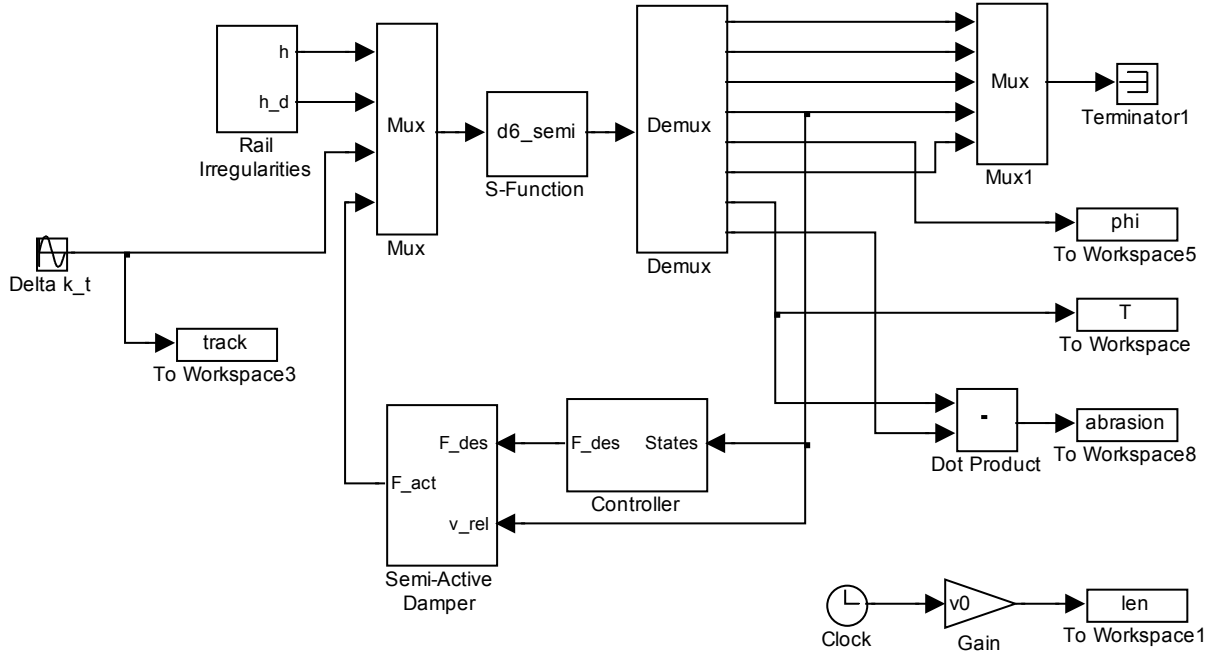


Figure 9: Simulink block diagram of a model with semi-active sleepers

4.1.1 Model of Semi-Active Damping Device

The most important modification is the application of the semi-active damping device. In this case, some simplifications are applied. The characteristics of the damping device are considered to be symmetric and linear (the damping ratio varies between b_{\min} and b_{\max}) and the dynamic behaviour caused by elasticity is neglected. It results in the following damping device law:

$$F_{act} = \left(b_{\min} + (b_{\max} - b_{\min}) \frac{i_{act}}{i_{\max}} \right) v_{rel}, \quad (12)$$

where

F_{act} is the actual output force,

b_{\min} is the minimal damping ratio,

b_{\max} is the maximal damping ratio,

i_{act} is the actual current between 0 and i_{\max}

i_{\max} is the maximal damping device current, and

v_{rel} is the relative damping device velocity.

The Simulink implementation of a semi-active damping device model is presented in Figure 10.

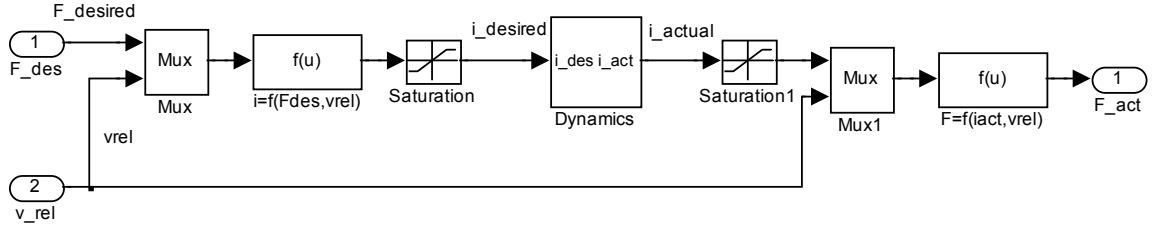


Figure 10: Simulink block diagram of a semi-active damping device model

4.2 Controller and Its Optimisation

The selection of sensors has a significant influence on the controller structure. The first experiments have been performed with so-called acceleration feedback, see e.g. [11]. This concept is simple and feasible. It requires measuring vertical acceleration only:

$$F_{des} = k_{opt} \ddot{z}_t, \quad (13)$$

where

F_{des} is the desired force,

k_{opt} is the controller gain, and

\ddot{z}_t is the rail acceleration.

In order to optimise the controller, an optimisation method should be selected. There are many criteria for the selection of a proper optimisation algorithm. Since because of the nonlinearities more than one local minimum is expected, a global optimisation method should be chosen. Since analytic gradient functions are not available in this case, methods based on evaluation function values only are preferable. A further criterion is availability. The method should be simply implementable to MATLAB, or already available.

The Multilevel Coordinate Search method which MATLAB implementation MSC is available has been chosen to optimise such a nonlinear system which balances global and local search. This method is designed for bound constrained global optimisation using function values only. The local search is done by using sequential quadratic programming. A derivation of the algorithm, the underlying theory, and numerical comparisons can be found e.g. in [12].

Maximal value of abrasion rate between the 5th and 7th meter is chosen as an optimisation criterion. However, this criterion does not seem to be ideal because it reduces the long waves, but the short waves still could remain.

4.3 Simulation Results

The simulation results proved that the controlled semi-active sleeper has a contribution to the reduction of the corrugation formation. The simulation indicates that the controlled sleepers have potential to reduce the abrasion by about 75 % for the selected model, see Figure 11.

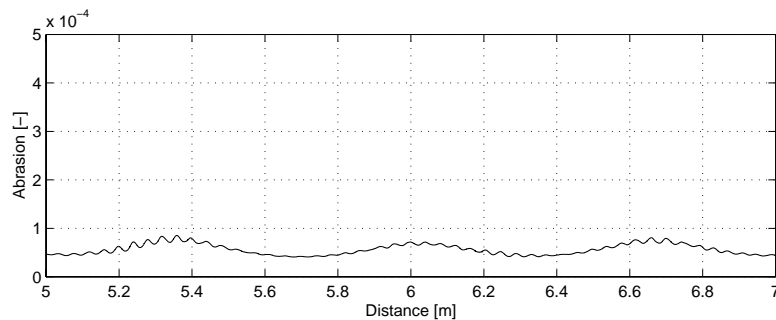


Figure 11: Abrasion rate for the semi-active track

As expected from the criteria definition, in this case particularly the long waves are suppressed. The amplitude of the short waves remains. It can also be explained by the dynamics of the semi-active damping device which is not able to act in such high frequencies.

5 CONCLUSIONS AND OPEN PROBLEMS

This paper presented one of the possible applications of semi-active actuators for reducing the corrugation of rails.

The proper corrugation mechanism is not well understood. It seems to be specific for a given track and vehicle. The corrugation occurs as a result of the longitudinal slip between wheel and rail and the variation of track impedance. Some eigenmodes of the vehicle-track system are excited which result to the corrugation wear.

The simulation results indicate that corrugation is caused by several factors. In curves and braking and traction areas slip with high creepage forces is present. The eigenmodes of the wheelset are excited, particularly the torsional eigenmodes are important. The process is initiated by rail irregularities and further encouraged by track impedance variation. It is also observed that the track without impedance variation (i.e. continuously supported track) results in a significant reduction of corrugation.

Finally, the application of semi-active sleepers is proposed. The semi-active track is expected to be applied only in the most critical areas, e.g. in low radius curves. Simple and feasible control law has been applied. The study shows that controlled semi-active tracks have potential for reducing the corrugation. The main question is the feasibility of the proposed semi-active sleepers. However, the modification of the selected critical parts of the tracks seems to be more feasible than the re-design of the existing vehicle fleet. This

advantage is even emphasised by the fact that the rolling stock and the railway maintenance are in many cases split between different companies.

The model presented in this paper is simplified, but it includes essential features of corrugation formation. However, the advanced models of elastic wheelsets and rail which are recently available, [13], are a very good basis for further more detailed investigations.

ACKNOWLEDGEMENTS

The authors acknowledge Brussels-Capital Region for supporting this research in project Research in Brussels RIB 1998 - 007.

REFERENCES

- [1] G. Diana, F. Cheli, S. Bruni, and A. Collina. Experimental and numerical investigation on subway short pitch corrugation. In L. Palkovics, editor, *The Dynamics of Vehicles on Roads and on Tracks*, Supplement to Vehicle System Dynamics, Volume 29, pages 234 - 245. Swets & Zeitlinger, 1998.
- [2] S.L. Grassie and J.A. Elkins. Rail corrugation on north american transit system. In L. Palkovics, editor, *The Dynamics of Vehicles on Roads and on Tracks*, Supplement to Vehicle System Dynamics, Volume 29, pages 5 - 17. Swets & Zeitlinger, 1998.
- [3] B. Ripke and K. Hepelmann. Model prediction of track loads and rail corrugation. *Railway Gazette International*, pages 447 - 450, July 1994.
- [4] O. Vaculín. Semi-active suspension of railway vehicles. Research in Brussels RIB - 1998/007 Final Report, ULB, Brussels, 1999.
- [5] V. Stejskal and M. Valášek. *Kinematics and Dynamics of Machinery*. Marcel Dekker, Inc., New York, 1996.
- [6] M. Valášek, V. Stejskal, Z. Šika, O. Vaculín, and J. Kovanda. Dynamic model of truck for suspension control. In L. Palkovics, editor, *The Dynamics of Vehicles on Roads and on Tracks*, Supplement to Vehicle System Dynamics, Volume 29, pages 717 - 722. Swets & Zeitlinger, 1998.
- [7] DLR, Oberpfaffenhofen. *SIMPACT - User Manual*, 1995.
- [8] E. Brommundt. Polygonization of a single rolling wheel by wear. In *EUROMECH - 2nd European Nonlinear Oscillation Conference*, pages 101 - 104, Prague, Czech Republic, 1996.
- [9] S. Iwnicki. The manchester benchmark for rail simulators - an introduction. In L. Palkovics, editor, *The Dynamics of Vehicles on Roads and on Tracks*, Supplement to Vehicle System Dynamics, Volume 29, pages 717 - 722. Swets & Zeitlinger, 1998.
- [10] A. Powell. On the dynamics of actively steered railway vehicles. In L. Palkovics, editor, *The Dynamics of Vehicles on Roads and on Tracks*, Supplement to Vehicle System Dynamics, Volume 29, pages 506 - 520. Swets & Zeitlinger, 1998.
- [11] R. Hölscher and Z. Huang. Das komfortorientierte semiaktive DÄamfungssystem. In H. Wallentowitz, editor, *Fortschritte der Fahrzeugtechnik 10, Aktive Fahrwerkstechnik*. Vieweg Verlag, 1991.

- [12] W. Huyer and A. Neumaier. *Global optimization by multilevel coordinate search*. *Journal of Global Optimization*, 14, pages 331 - 355, 1999.
- [13] K. Popp, I. Kaiser, and H. Kruse. System dynamics of railway vehicles and tracks. *Archive of Applied Mechanics*, 72(11-12):949 - 961, 2003.